

Additional J/Ψ suppression from high density effects

M.B. Gay Ducati^{1,a}, V.P. Gonçalves^{2,b}, L.F. Mackedanz^{1,c}

¹ Instituto de Física, Universidade Federal do Rio Grande do Sul, Caixa Postal 15051, CEP 91501-970, Porto Alegre, RS, Brazil

² Instituto de Física e Matemática, Universidade Federal de Pelotas, Caixa Postal 354, CEP 96010-090, Pelotas, RS, Brazil

Received: 10 October 2003 / Revised version: 23 December 2003 /

Published online: 25 February 2004 – © Springer-Verlag / Società Italiana di Fisica 2004

Abstract. At high energies the saturation effects associated to the high parton density should modify the behavior of the observables in proton–nucleus and nucleus–nucleus scattering. In this paper we investigate the saturation effects in the nuclear J/Ψ production and estimate the modifications in the energy dependence of the cross section as well as in the length of the nuclear medium. In particular, we calculate the ratio of J/Ψ to Drell–Yan cross sections and show that it is strongly modified if the high density effects are included. Moreover, our results are compared with the data from the NA50 Collaboration and predictions for the RHIC and LHC kinematic regions are presented. We predict an additional J/Ψ suppression associated to the high density effects.

1 Introduction

High energy heavy-ion collisions offer the opportunity to study the properties of the predicted QCD phase transition to a locally deconfined quark–gluon plasma (QGP) (see, e.g., [1]). A dense parton system is expected to be formed in the early stage of relativistic heavy-ion collisions at RHIC (Relativistic Heavy Ion Collider) energies and above, due to the onset of hard and semihard parton scatterings. The search for experimental evidence of this transition during the very early stage of AA reactions requires one to extract unambiguous characteristic signals that survive the complex evolution through the later stages of the collision. One of the proposed signatures of the QCD phase transition is the suppression of quarkonium production, particularly of the J/ψ [2]. The idea of suppression of $c\bar{c}$ mesons J/ψ , ψ , etc., is based on the notion that $c\bar{c}$ are produced mainly via primary hard collisions of energetic gluons during the preequilibrium stage up to shortly after the plasma formation (before the initial temperature drops below the production threshold), and the mesons formed from these pairs may subsequently experience deconfinement when traversing the region of the plasma. In a QGP, the suppression occurs due to the shielding of the $c\bar{c}$ binding potential by color screening, leading to the breakup of the resonance. The $c\bar{c}$ ($J/\psi, \psi', \dots$) and $b\bar{b}$ ($\Upsilon, \Upsilon', \dots$) resonances have smaller radii than light-quark hadrons and therefore higher temperatures are needed to dissociate these quarkonium states.

Over the years, several groups have measured the J/Ψ yield in heavy-ion collisions with the J/Ψ suppression observed in the experimental data. In particular, the NA50 Collaboration at CERN observed a much stronger J/Ψ suppression in Pb–Pb collisions at SPS energies [3]. Different mechanisms have been proposed to explain this phenomenon. It has been suggested that the suppression was due the QGP phase [4], percolation deconfinement [5] or absorption by comovers [6,7] (for a review see e.g. [8]). Recently, the origin of the anomalous behavior of the J/Ψ production cross section has still been debated and several competing interpretations have so far been proposed. In general, these models consider the final state interactions of the quarkonium state with the nuclear/QGP medium. A comprehensive analysis of the different mechanisms is presented in [9]. Here, we address another search of J/Ψ suppression in nuclear collisions at high energies: the modification in the nuclear wave functions of the incident nuclei associated to the high density (saturation) effects.

The probability of a thermalized QGP production and the resulting strength of its signatures strongly depends on the initial conditions associated to the distributions of partons in the nuclear wave functions. At very high energies, the growth of parton distributions should saturate. There is a possible formation of a color glass condensate [10], characterized by a bulk momentum scale Q_s . Moreover, the limitation on the maximum phase-space parton density that can be reached in the hadron wave function (parton saturation) and very high values of the QCD field strength squared $F_{\mu\nu}^2 \propto 1/\alpha_s$ [11] are expected in this regime. Furthermore, the number of gluons per unit phase-space volume practically saturates and at large densities grows only very slowly (logarithmically) as a function of the energy [12]. If the saturation scale is larger than the

^a e-mail: gay@if.ufrgs.br

^b e-mail: barros@ufpel.edu.br

^c e-mail: thunder@if.ufrgs.br

QCD scale A_{QCD} , then this system can be studied using weak coupling methods. The magnitude of Q_s is associated to the behavior of the gluon distribution at high energies, and some estimates have been obtained. In general, the predictions are $Q_s \sim 1$ GeV at RHIC and $Q_s \sim 2-3$ GeV at LHC [13,14]. From the experimental point of view, the recent results from HERA for ep collisions [15,16] and from RHIC for heavy-ion collisions [17–19] suggest that these processes at high energies probe QCD in the non-linear regime of high parton density. These results motivate our analysis of the J/Ψ production in nuclear processes.

In this work, we analyze in detail the J/Ψ production in pA and AA processes. A detailed study of the J/Ψ production in pA collisions is justified by the fact that a systematic study of pA and AA scatterings at the same energies is essential to gain insight into the structure of the dense medium effects. Such effects, as the energy loss and high density effects, are absent or small in pp collisions, but become increasingly prominent in pA collisions, and are of major importance in AA reactions. By comparing pA and AA reactions involving very heavy nuclei, one may be able to distinguish basic hadronic effects that dominate the dynamics in pA collisions, from a quark–gluon formation predicted to occur in heavy-ion AA collisions. Furthermore, our analysis is motivated by the fact that the quarkonium production at RHIC and LHC energies is dominated by initial state gluons. As the probability for making a heavy quark pair is proportional to the square of the gluon distribution, any depletion in number of gluons will make a significant difference in the number of the J/Ψ produced [20]. Here we assume the presence of initial state effects in the nuclear wave functions and final state interactions of the $c\bar{c}$ pair with the nuclear medium. Our main goal is to estimate the magnitude of quarkonium suppression in hadronic matter associated to these effects. Our results demonstrate that the high density effects imply an additional J/Ψ suppression when compared with the scenario where only final state interactions are estimated. As the formation of a QGP is not assumed, our predictions are a lower bound for the J/Ψ suppression in high energy nuclear collisions.

This paper is organized as follows. In the next section, we present the color evaporation model (CEM), which is used as a model for the J/Ψ production in proton–nucleus (pA) and nucleus–nucleus (AA) collisions. In Sect. 3 we present a brief review of the AG parameterization [21], used to include the high density effects in the calculation. Moreover, we present our predictions for the energy dependence of the J/Ψ cross section in Sect. 4. In Sect. 5 the generalization of the CEM to the inclusion of the final state interactions proposed in [22] is discussed and our results for the medium length dependence of the cross sections are presented in Sect. 6. Our main conclusions are also summarized.

2 J/Ψ production in the collinear factorization

Vector-meson production has proven to be a very interesting process in which one may test the interplay between the perturbative and non-perturbative regimes of QCD (for a review, see for example [23,24]). One of the main uncertainties in quarkonium production is related to the transition from the colored state to a colorless meson. Initially, the $q\bar{q}$ pair will in general be in a color octet state. It subsequently neutralizes its color and binds into a physical resonance. Color neutralization occurs by interaction with the surrounding color field. An alternative view of the J/Ψ production process is to use the color evaporation model (CEM), which describes a large range of data in hadro- and photoproduction, as shown in [25]. In CEM, quarkonium production is treated identically to open heavy quark production with the exception that, in the case of quarkonium, the invariant mass of the heavy quark pair is restricted to be below the open meson threshold, which is twice the mass of the lowest meson mass that can be formed with the heavy quark. For charmonium the upper limit on the $c\bar{c}$ mass is then $2m_D$. The hadronization of the charmonium states from the $c\bar{c}$ pairs is non-perturbative, usually involving the emission of one or more soft gluons. Depending on the quantum numbers of the initial $c\bar{c}$ pair and the final state charmonium, a different matrix element is needed for the production of the charmonium state. The averages of these non-perturbative matrix elements are combined into the universal factor $F[nJ^{PC}]$, which is process- and kinematics-independent and describes the probability that the $c\bar{c}$ pair binds to form a quarkonium $J/\Psi(nJ^{PC})$ of given spin J , parity P , and charge conjugation C . Once F has been fixed for each state (J/Ψ or Ψ') the model successfully predicts the energy and momentum dependence [26,27].

Considering the J/Ψ production and the collinear factorization approach, the CEM predicts that the cross section in the collision of hadrons A and B is given by

$$\sigma_{AB \rightarrow J/\psi X} = K \sum_{a,b} \int dq^2 \left(\frac{\hat{\sigma}_{ab \rightarrow c\bar{c}}(Q^2)}{Q^2} \right) \quad (1)$$

$$\times \int dx_F \phi_{a/A}(x_a) \phi_{b/B}(x_b) \frac{x_a x_b}{x_a + x_b} F_{c\bar{c} \rightarrow J/\psi}(q^2),$$

where $\sum_{a,b}$ runs over all parton flavors, $Q^2 = q^2 + 4m_c^2$, $\phi_{a/A}(x_a)$ is the distribution function of parton a in hadron A , $x_F = x_a - x_b$ and $x_a x_b = Q^2/s \equiv \tau$. The expressions of the elementary partonic cross sections can be taken from [28], and to take into account the next-to-leading order corrections to the cross section we consider the phenomenological constant K -factor. The factor $F_{c\bar{c} \rightarrow J/\psi}(q^2)$ describes the transition probability for the $c\bar{c}$ state of the relative square momentum q^2 to evolve into a physical J/ψ meson. In general, it is parameterized by

$$F_{c\bar{c} \rightarrow J/\psi}(q^2) = N_{J/\psi} \theta(q^2) \theta(4m_D^2 - 4m_c^2 - q^2), \quad (2)$$

where $N_{J/\psi}$ is a normalization factor which is obtained from a fit of the experimental data for J/Ψ produc-

tion in proton–proton collisions. Here, we assume that $KN_{J/\Psi} = 0.250$, similarly to what is done in [22,25], where this model was successfully compared with the experimental results. For nuclear collisions, a number of experiments has measured a less than linear A dependence for various processes of production [29,30], which indicates that the nuclear medium effects cannot be disregarded.

3 High density effects in J/Ψ production

One important point for the studies of J/Ψ production is that in the J/Ψ cross section calculation using the collinear factorization framework we integrate over the momentum fraction of the incoming partons. This implies that we must know the behavior of the nuclear parton distributions in the full x range to obtain realistic predictions for these observable. The current estimates for the nuclear J/Ψ production (see e.g. [31]) consider as input the EKS parameterization for the nuclear parton distributions [32], which are solutions of the DGLAP evolution equations [33]. Consequently, these analyses do not consider the possible presence of high density effects which should modify the dynamical evolution of the nuclear parton distributions in the RHIC and LHC kinematical regions.

As our focus is to analyze the influence of the high density effects in the J/Ψ production, here we only consider the medium modifications in the nuclear parton distributions (nuclear shadowing effect), disregarding the contributions of energy loss and the intrinsic heavy quark components for the non-linear A dependence of the cross sections (for a discussion of these effects in charmonium production, see [34]). The nuclear shadowing is the modification of the nuclear parton distributions so that $\phi_{a/A}(x, Q^2) \neq \phi_{a/p}(x, Q^2)$, as expected from a superposition of pp interactions. The current experimental data presenting nuclear shadowing can be described reasonably well using the DGLAP evolution equations [33] with adjusted initial parton distributions [32]. However, this parameterization does not include the dynamical saturation effects predicted to modify the evolution equation and, consequently, the behavior of the nuclear parton distributions at small x and large A [11]. In this kinematical regime, the density of quarks and gluons becomes very high and the processes of interaction and recombination between partons, not present in the DGLAP evolution, should be considered.

Therefore, in order to investigate the presence and magnitude of the high density effects in the nuclear J/Ψ production considering the collinear factorization of the cross section, it is necessary to include these effects, as well as the antishadowing, EMC and Fermi motion effects, in the nuclear parton distributions. Here we use as input in our calculations the AG parameterization proposed in [21], which improves the EKS one by the inclusion of the perturbative high density effects [35]. This parameterization deals with these effects using the Glauber–Mueller formula, which is the simplest one that reflects the main qualitative features of a more general approach based on non-linear evolution [10,36]. For completeness, we now

present a qualitative discussion of the main properties of the approach used by this parameterization.

In the nucleus rest frame we can consider the interaction between a virtual colorless hard probe and the nucleus via the gluon pair (gg) component of the virtual probe. The interaction of the dipole with the color field of the nucleus will clearly depend on its size. If the separation of the gg pair is very small (smaller than the mean separation of the partons), the color field of the dipole will be effectively screened and the nucleus will be essentially transparent to the dipole. At large dipole sizes, the color field of the dipole is large and it interacts strongly with the target and is sensitive both to its structure and size. More generally, when the parton density is such that the nucleus becomes black and the interaction probability is unity, the dipole cross section saturates and the gluon distribution becomes proportional to the virtuality of the probe Q^2 . In the infinite momentum frame, this picture is equivalent to a situation in which the individual partons become so close that they have a significant probability of interacting with each other before interaction with the probe. Such interactions lead, for instance, to two \rightarrow one branchings and hence a reduction in the gluon distribution. These properties were considered in [35], where the rescatterings of the gluon pair inside the nucleus were estimated using the Glauber–Mueller approach, with the result that the nuclear gluon distribution is given by

$$xG_A(x, Q^2) = \frac{2R_A^2}{\pi^2} \int_x^1 \frac{dx'}{x'} \int_{\frac{1}{Q^2}}^{\frac{1}{Q_0^2}} \frac{d^2r_t}{\pi r_t^4} \times \{C + \ln(\kappa_G(x', r_t^2)) + E_1(\kappa_G(x', r_t^2))\}, \quad (3)$$

where C is the Euler constant, E_1 is the exponential function, the function $\kappa_G(x, r_t^2) = (3\alpha_s A/2R_A^2) \pi r_t^2 xG_N(x, \frac{1}{r_t^2})$, A is the number of nucleons in a nucleus and R_A^2 is the mean nuclear radius. The limit of low densities is characterized by $\kappa_G \ll 1$, while for high parton densities $\kappa_G \gg 1$. The transition line between these two regimes can be obtained assuming $\kappa_G = 1$ [37], which allows us to estimate the saturation momentum scale Q_s^2 . One of the shortcomings of this approach is that the Glauber–Mueller formula does not contemplate any nuclear effect in the non-perturbative initial condition for the gluon distribution. The antishadowing and EMC effects present at larger values of x are also disregarded in this approach. In order to improve this approach, there was proposed in [21] a modification in the expression (3) which includes the full DGLAP kernel in parton evolution. Basically, to calculate the nuclear gluon distribution the following procedure was proposed:

$$xG_A(x, Q^2) = (1/A)xG_A(x, Q^2)[\text{GM}] - (1/A)xG_A(x, Q^2)[\text{DLA}] + xG_A(x, Q^2)[\text{EKS}], \quad (4)$$

where $xG_A(x, Q^2)[\text{GM}]$ represents the Glauber–Mueller nuclear gluon distribution given by the expression (3) and $xG_A(x, Q^2)[\text{DLA}]$ is the DGLAP (DLA) prediction for the nuclear gluon distribution, which corresponds to the first

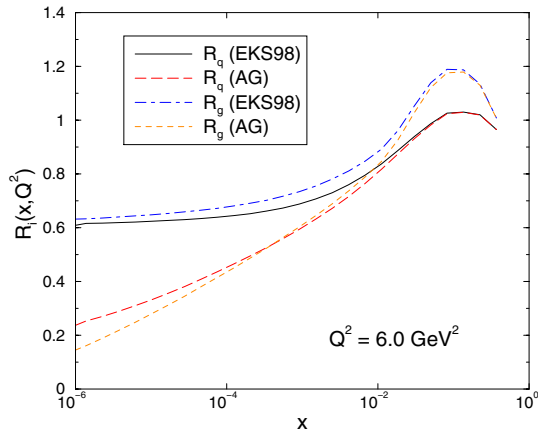


Fig. 1. The x dependence of the nuclear ratios R_g and R_q ($Q^2 = 6.0 \text{ GeV}^2$)

term of expression (3) when expanded in powers of κ_G . The last term in expression (4), $xG_A(x, Q^2)$ [EKS], is the gluon distribution solution of the DGLAP equation as proposed in [32], where the initial conditions of the parton evolution were chosen in such a way to describe the nuclear effects in DIS and Drell–Yan fixed nuclear target data. As it was discussed in detail in [21], the parameterization of the nuclear effects in the gluon distribution, given by the ratio $R_g(x, Q^2) = xG_A(x, Q^2)/xG_N(x, Q^2)$ in the EKS procedure, does not include the perturbative high density effects at small values of x associated to the QCD dynamics in this regime. Thus, the procedure presented in (4) includes the full DGLAP evolution equation in the whole kinematic region, taking into account the nuclear effects in the present fixed target data and high density effects in the parton evolution at small x in the perturbative regime. A similar procedure can be implemented to obtain the nuclear quark distribution [38]. In Fig. 1 we present the predictions for the x dependence of nuclear ratios R_g and $R_q = xq_A/xq_N$ considering the high density effects. The predictions of the EKS parameterization are also shown for comparison. Two points must be emphasized:

- (a) at small values of x the difference between the AG and EKS predictions are very large and merits our consideration;
- (b) the effects for gluons are larger than for quarks.

This last result has strong implications in the calculations of the ratio between the J/Ψ and Drell–Yan cross sections, as will be demonstrated in that follows. A comment is in order here. Currently, there is a large uncertainty related to the behavior of the nuclear parton distributions at small values of x . As discussed in [39], the distinct models present in the literature agree within 15% for $x \approx 0.01$, where experimental data exist, while they differ up to 60% in its predictions for $R_{F_2} = F_2^A/F_2^N$ at $x = 10^{-5}$. Our prediction for this ratio using the AG parameterization is identical to the EKS results for large x and very similar to the eikonal one obtained in [39]. Therefore, we believe that the approach used here can be considered as a suitable phenomenological method for the

inclusion of the high density effects in the nuclear cross sections at RHIC and LHC energies. Clearly, for higher values of the parton density, a more general framework should be considered for the calculations of the cross sections (see e.g. [40]).

4 Energy dependence for J/Ψ production

In order to investigate the medium dependence of the J/Ψ production cross section due to high density effects, we will follow the usual procedure to describe the experimental data on nuclear effects in the hadronic quarkonium production [30], where the atomic mass number A dependence is parameterized by $\sigma_{pA} = \sigma_{pN} \times A^\alpha$. Here, σ_{pA} and σ_{pN} are the particle production cross sections in proton–nucleus and proton–nucleon interactions, respectively. If the particle production is not modified by the presence of nuclear matter, then $\alpha = 1$. In Fig. 2 we present the effective exponent α as a function of the CM energy $s^{1/2}$, where we have calculated the J/Ψ cross section using the EKS and AG parameterizations as input in our calculations. In both cases, we assume that the nucleon parton distributions are given by the GRV94(LO) set [41]. The general behavior of the exponent can be understood as follows: when the integrations in (1) are taken, the nuclear gluon distributions are evaluated in the x_2 interval given by $\tau < x_2 < \sqrt{\tau}$. Thus, when the energy grows, the x_2 interval goes to the small x region. For J/Ψ production, for example, the antishadowing region dominates the integration for energies smaller than 80 GeV. For larger values of energy, the suppression is sizeable and the effective exponent is smaller than 1. On general grounds, we have that the exponent observed in the EKS prediction almost saturates and it is associated to the behavior of the ratio R_g at small x , while the presence of the high density effects (non-saturation of R_g) implies a large reduction of the pA cross section when compared with DGLAP-EKS description of nuclear effects. Therefore, we believe that the analysis of the effective exponent in pA processes can be useful to make clear the high density effects.

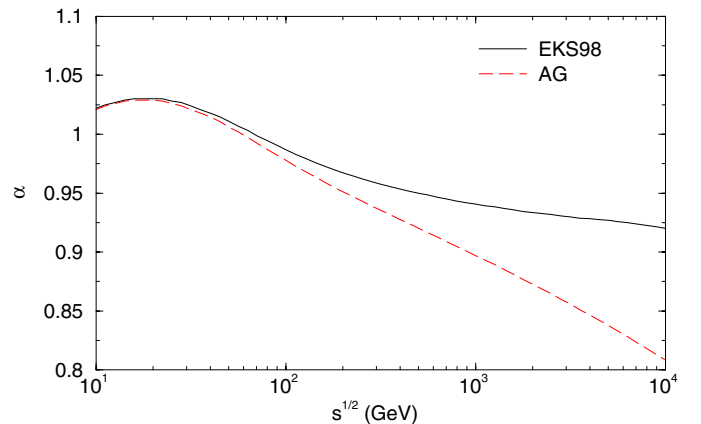


Fig. 2. Energy dependence of the effective exponent α for J/Ψ production in pA processes

In general, the experimental analysis of the J/Ψ suppression [3] considers as baseline the study of the ratio between J/Ψ and Drell–Yan (DY) cross sections. However, to make the suppression of this ratio an unambiguous test, we must consider all possible effects present in the production cross sections. In particular, we cannot disregard the high density effects in the nuclear quark distributions and the larger magnitude of these effects in the nuclear gluon distribution. In Fig. 3 we present our results for the energy dependence of the ratio $\sigma_{J/\Psi}/\sigma_{DY}$ for pA (top panel) and AA processes (bottom panel). For the calculation of the Drell–Yan cross section we include the high density effects in the nuclear quark distributions [38]. As these effects are larger in the gluon case, the ratio will be strongly modified when compared to the calculations without the inclusion of the high density effects. We verify that this modification is already present in pA process at RHIC energy, and is almost 40% for LHC energies, which implies that this process could be used to identify the presence and estimate the magnitude of the high density effects. Moreover, we predict a large suppression of the quarkonium production in AA processes, associated with the presence of these effects, independently of the production of a quark–gluon plasma. As the additional suppression of the charmonium production rate predicted here is associated to the distinct dependence of the J/Ψ and Drell–Yan cross sections in the nuclear parton distributions, one alternative analysis is to use as baseline the ratio $\sigma_{J/\Psi}/\sigma_{Q\bar{Q}}$ between the bound and open states cross section [42]. Since both processes similarly depend on the nuclear gluon distribution, this ratio is weakly dependent on the inclusion of the high density effects [43].

It is important to emphasize that the description of the J/Ψ production using collinear factorization at RHIC and LHC is still an open question. At large energies the replacement of the collinear factorization by the k_{\perp} -factorization formalism is expected (for a recent review see, e.g., [44]). Moreover, coherence effects may lead to a breakdown of the collinear factorization [45], implying that dynamical effects, such as shadowing, may become process dependent. In this work, we choose a more conservative approach for the treatment of the J/Ψ production. We assume as valid the collinear factorization and, in particular, the color evaporation model, and consider that the high density effects only modify the nuclear parton distributions. Moreover, we assume that initial and final state effects can be separated and consider different approaches for these distinct phases. The current experimental data for particle production at large transverse momentum for $\sqrt{s} = 200$ GeV has demonstrated that this approach is valid at least for RHIC energies. We believe that our analysis can be considered as a lower bound for the magnitude of the high density effects in J/Ψ production, since the Glauber–Mueller approach considered here is one of the limits of the color glass condensate for intermediate values of the parton density. Clearly, for higher values of the energy, a more general framework should be considered in the calculations of the quarkonium cross section.

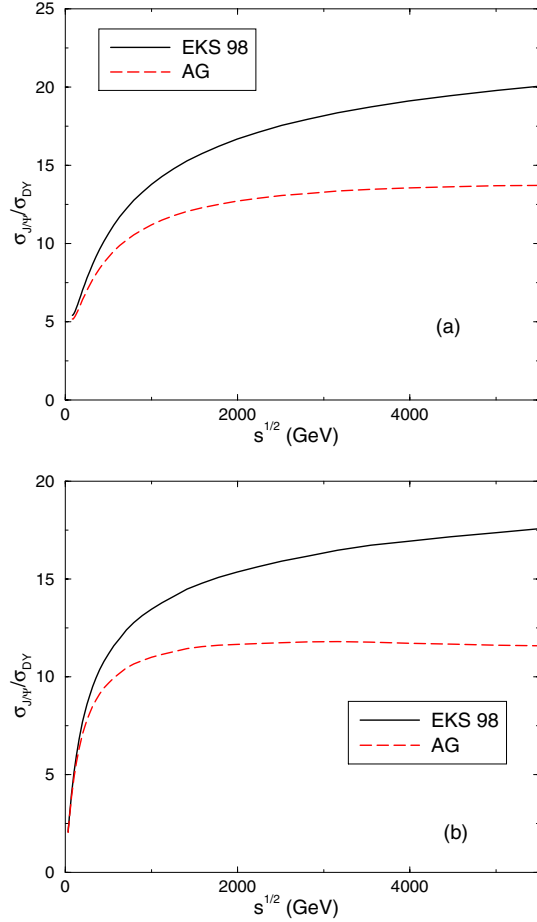


Fig. 3. Energy dependence of the ratio between the J/Ψ and DY cross sections for **a** pA and **b** AA collisions

5 Final state interactions

In the later section we have demonstrated that the inclusion of the high density effects implies an additional suppression of the J/Ψ production rate. However, a complete description of nuclear J/Ψ production requires a proper treatment of both the initial state modifications of the parton distributions and the final state interactions of the produced $c\bar{c}$ pairs. Therefore, in order to obtain a more realistic prediction for the J/Ψ suppression in heavy-ion collisions, we must include the final state interactions. Here, we will consider the model recently proposed in [22] (see also [46]), where the CEM is generalized to include the multiple scatterings between the $c\bar{c}$ and soft gluons as the pair crosses the nuclear medium. In this model, the $c\bar{c}$ is produced with a separation smaller than the J/Ψ radius. Besides, the energy exchanges in the collisions are greater than the non-perturbative momentum scales in the J/Ψ wave function. Following this, the meson is unlikely to be formed at the collision point and the transformation from a pre-resonant $c\bar{c}$ into a physical J/Ψ may occur over several Fermi [47]. During this transformation, the produced $c\bar{c}$ pair interacts via multiple scatterings with the spectators of the collision [48]. As a consequence of the multiple scattering, the square of the relative momen-

tum q^2 between the $c\bar{c}$ pair is increased, and some of the $c\bar{c}$ pairs could gain enough q^2 to reach the threshold for open charm production. As a result, the cross sections for J/Ψ production is reduced in comparison with nucleon–nucleon collisions.

In the QVZ model [22], the transition probability $F_{c\bar{c}\rightarrow J/\Psi}(q^2)$, present in (1), is parameterized by

$$F_{c\bar{c}\rightarrow J/\Psi}(q^2) = N_{J/\Psi} \theta(q^2) \theta(4m_D^2 - 4m_c^2 - q^2) \times \left(1 - \frac{q^2}{4m_D^2 - 4m_c^2}\right)^{\alpha_F}, \quad (5)$$

where the gluon radiation effect is simulated by the parameter $\alpha_F > 0$, which puts larger weight to the smaller q^2 . Furthermore, the QVZ model additionally assumes that the multiple scattering of the pair in the nuclear medium would increase the relative square momentum q^2 of the pair. The effect of coherent multiple scattering in the perturbative QCD calculation may be represented by shifting of the relative momentum in the transition probability as follows [22]:

$$F_{c\bar{c}\rightarrow J/\Psi}(\bar{q}^2) = F_{c\bar{c}\rightarrow J/\Psi}(q^2 + \epsilon^2 L), \quad (6)$$

where L is the effective length of the nuclear medium in the AB collisions and ϵ^2 is the squared relative momentum gained by the produced $c\bar{c}$ pair per unit length. The above behavior implies that for a large enough L , such that for $\bar{q}^2 > 4m_D^2 - 4m_c^2$, the transition probability essentially vanishes due to the existence of the open charm threshold. This gives rise to a much stronger suppression than the exponential one following from the Glauber model [49]. In principle, the uniform shift of the relative momentum may be obtained in a perturbative QCD calculation by summing up all twist contributions at the leading order in the strong coupling constant α_s and the nuclear size [50]. As shown in [22], the model describes all observed J/Ψ suppression data in hadron–nucleus and nucleus–nucleus collisions if the parameters α_F and ϵ are fitted. Moreover, the model is weakly dependent of the value of α_F , which is not true for ϵ^2 . It is important to emphasize that the authors have disregarded the effects in the nuclear parton distributions in the calculations. Below, we demonstrate that the inclusion of these effects is important for the SPS energies and should be included in the future predictions for RHIC and LHC energies.

6 Results and conclusions

In the later sections we have presented the model to treat the medium effects in nuclear collisions. In Sect. 3, we have discussed the initial state effects, and in Sect. 5, we have presented a model to treat the final state effects, and its implications for the J/Ψ suppression. In this section, we present our results for J/Ψ production, when these effects are considered. Since we are interested in the magnitude of the suppression due to high density effects, we present the results for total cross sections for charmonium productions, assuming that only the small x_F region will be accessible at RHIC and LHC.

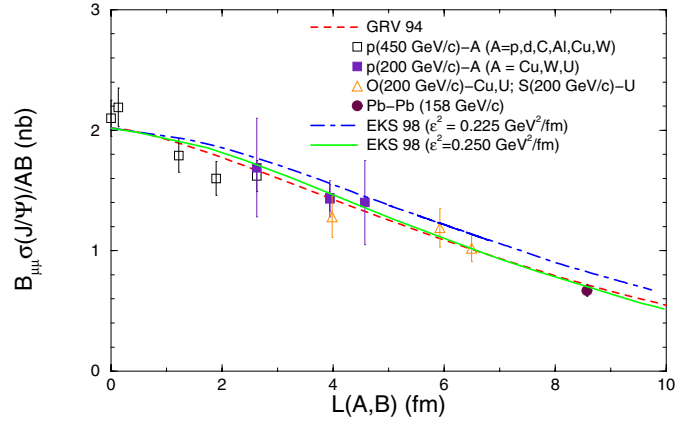


Fig. 4. Total J/Ψ cross sections with the branching ratios to $\mu^+\mu^-$ in pA and AA collisions, as a function of the effective nuclear length $L(A, B)$

In Fig. 4 we show our results for the medium length dependence of the J/Ψ cross section. The effective length $L(A, B)$, as well as the experimental data, are taken from the [3], with all data rescaled to $P_{\text{beam}} = 200$ GeV. Following [22], we assume $KN_{J/\Psi} = 0.458$. The dashed line is our prediction obtained using the GRV94 parameterization and, as done in [22,46], we assume $\epsilon^2 = 0.225$ GeV²/fm. In this case we are disregarding any nuclear effects present in the parton distributions. If these nuclear effects are considered, we obtain the dash-dotted curve, where we kept $\epsilon^2 = 0.225$ GeV²/fm and used the EKS parameterization. It can be seen that if these effects are included the model fails to describe the Pb–Pb data. This behavior is associated to the antishadowing effect present in the EKS nuclear parton distribution, which implies an enhancement of the cross section, and more scatterings between the $c\bar{c}$ pair and the medium are necessary to describe the data. This situation can be improved using the fact that ϵ^2 , the gained momentum per unit length, is a free parameter of the model. In the solid line we show our prediction using $\epsilon^2 = 0.250$ GeV²/fm, which improves the description. This modification in the parameter demonstrates that the inclusion of the medium effects are important for SPS energies. It is important to emphasize that our conclusions are unchanged if we use for comparison the latest NA50 data on J/Ψ production in pA and AA collisions [51]. As in the kinematical region of the experimental data the EKS and AG predictions for the nuclear parton distributions are identical, our predictions including the high density effects are not shown in the figure.

As we have determined a new value for the parameter ϵ^2 when the initial state medium effects are considered, we can use it to predict the nuclear J/Ψ production at higher energies. We assume that a QGP is not formed in these collisions. Consequently, our predictions are a lower bound for the J/Ψ suppression, since if this new state of matter is formed, another mechanism of suppression (deconfinement) not considered here is also present. In Fig. 5 we plot the our predictions for total cross sections for RHIC and

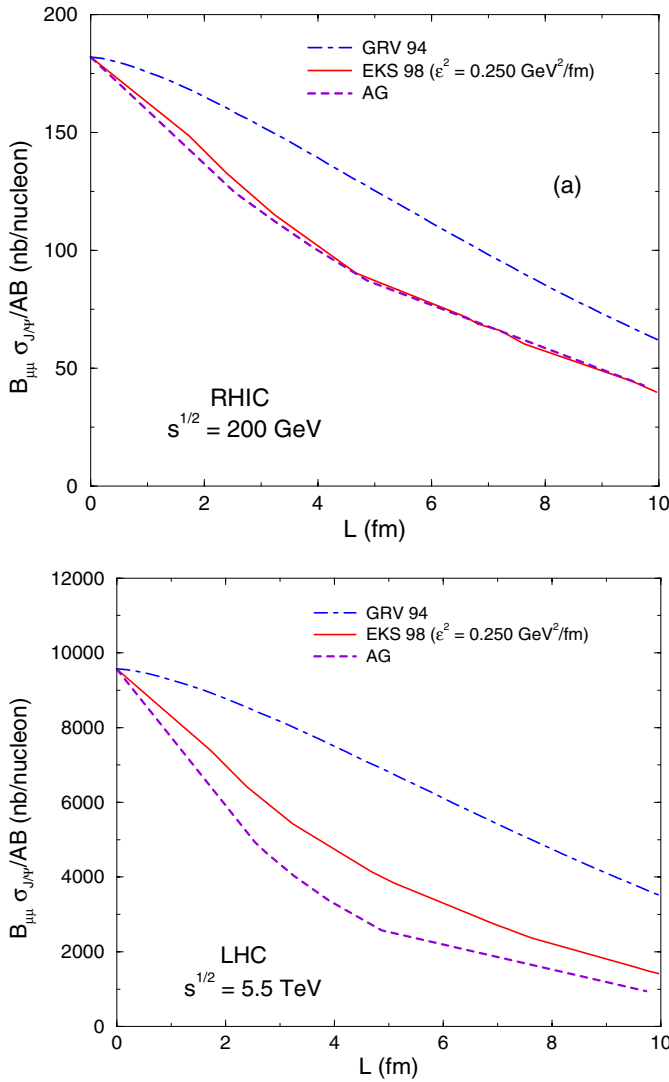


Fig. 5. The same as Fig. 4, for **a** RHIC and **b** LHC energies

LHC energies, using the GRV, EKS and AG parameterizations as input in our calculations. We can see by the comparison between the GRV and EKS curve that for the RHIC and LHC energies the medium effects present in the initial state cannot be disregarded, with the inclusion of these effects implying an additional J/Ψ suppression. Furthermore, for the kinematical region of RHIC the inclusion of the high density effects does not significantly modify the behavior of this observable. However, for LHC energies, we predict that these effects strongly reduce the J/Ψ production rate. This effect is associated to the dominance of the small- x behavior of the nuclear parton distributions at high energies.

A complete description of nuclear J/Ψ production requires a proper treatment of both the initial state modifications of the parton distributions and the final state interactions of the produced $c\bar{c}$ pairs. In this paper we have considered the inclusion of the high density effects in the parton distributions and estimated the J/Ψ cross section in pA and AA processes assuming that the collinear

factorization is still valid. Our results have demonstrated that these effects cannot be disregarded in the kinematical regions of the future colliders. In particular, we have shown that an additional J/Ψ suppression is expected if these effects are included in the calculations. As in AA collisions this suppression can also be associated to other sources, as for instance, comover interactions, percolation deconfinement or quark-gluon plasma formation, an experimental analysis of the J/Ψ production in pA processes at high energies is fundamental to constrain the hadronic effects. In particular, our results demonstrate that the high density effects will significantly contribute in the J/Ψ production in these processes, which implies that a careful disentangling of initial and final state effects is required before the clear identification of a new state of matter.

Acknowledgements. V.P.G. and L.F.M. are very grateful to A. Ayala Filho, M. A. Betemps and M. V. T. Machado for illuminating discussions on the subject. This work was partially financed by CNPq and FAPERGS, Brazil.

References

1. H. Satz, Nucl. Phys. A **715**, 3 (2003)
2. T. Matsui, H. Satz, Phys. Lett. B **178**, 416 (1986)
3. M.C. Abreu et al., Phys. Lett. B **477**, 28 (2000)
4. J.P. Blaizot, M. Dinh, J.Y. Ollitrault, Phys. Rev. Lett. **85**, 4012 (2000); Nucl. Phys. A **698**, 579 (2002)
5. N. Armesto, M. Braun, E.G. Ferreiro, C. Pajares Phys. Rev. Lett. **77**, 3736 (1996); S. Digo, S. Fortunato, P. Petreczky, H. Satz, Phys. Lett. B **549**, 101 (2002)
6. D. Kharzeev, H. Satz, Phys. Lett. B **334**, 155 (1994); B **356**, 365 (1995); B **366**, 316 (1996)
7. A. Capella, A.B. Kaidalov, D. Souza, Phys. Rev. C **65**, 054908 (2002); A. Capella, E.G. Ferreiro, A.B. Kaidalov, Phys. Rev. Lett. **85**, 2080 (2000)
8. R. Vogt, Phys. Rep. **310**, 197 (1999); H. Satz, Rep. Prog. Phys. **63**, 1511 (2000)
9. D. Kharzeev, C. Lourenco, M. Nardi, H. Satz, Z. Phys. C **74**, 307 (1997)
10. E. Iancu, A. Leonidov, L. McLerran, Nucl. Phys. A **692**, 583 (2001); E. Ferreiro, E. Iancu, A. Leonidov, L. McLerran, Nucl. Phys. A **703**, 489 (2002); E. Iancu, A. Leonidov, L. McLerran, hep-ph/0202270; E. Iancu, R. Venugopalan, hep-ph/0303204
11. A.H. Mueller, Nucl. Phys. B **558**, 285 (1999)
12. M.B. Gay Ducati, V.P. Gonçalves, Phys. Lett. B **502**, 92 (2001)
13. M. Gyulassy, L. McLerran, Phys. Rev. C **56**, 2219 (1997)
14. V.P. Gonçalves, Phys. Lett. B **495**, 303 (2000); M.B. Gay Ducati, V.P. Gonçalves, Phys. Lett. B **466**, 375 (1999)
15. K. Golec-Biernat, M. Wusthoff, Phys. Rev. D **59**, 014017 (1999); D **60**, 114023 (1999)
16. K.J. Eskola et al., Nucl. Phys. B **660**, 211 (2003)
17. D. Kharzeev, M. Nardi, Phys. Lett. B **507**, 121 (2001); D. Kharzeev, E. Levin, Phys. Lett. B **523**, 79 (2001); D. Kharzeev, E. Levin, M. Nardi, hep-ph/0111315
18. J. Schaffner-Bielich, D. Kharzeev, L. MacLerran, R. Venugopalan, Nucl. Phys. A **705**, 494 (2002)

19. A. Krasnitz, Y. Nara, R. Venugopalan, Nucl. Phys. A **717**, 268 (2003)
20. L.N. Epele, M.B. Gay Ducati, C.A. Garcia Canal, Phys. Lett. B **226**, 167 (1989)
21. A.L. Ayala Filho, V.P. Gonçalves. Eur. Phys. J. C **20**, 343 (2001); Phys. Lett. B **534**, 76 (2002)
22. J. Qiu, J.P. Vary, X. Zhang, Phys. Rev. Lett. **88**, 232301 (2002)
23. H. Abramowicz, A.C. Caldwell, Rev. Mod. Phys. **71**, 1275 (1999)
24. G.A. Schuler, CERN-TH 7170/94, hep-ph/9403387; E. Braaten, S. Fleming, T.C. Yuan, Ann. Rev. Nucl. Part. Sci. **46**, 197 (1996)
25. J.F. Amundson et al., Phys. Lett. B **372**, 127 (1996); M.B. Gay Ducati, C.B. Mariotto, Phys. Lett. B **464**, 286 (1999); M.B. Gay Ducati, G. Ingelman, C.B. Mariotto, Eur. J. Phys. C **23**, 527 (2002); M.B. Gay Ducati, V.P. Goncalves, C.B. Mariotto, Phys. Rev. D **65**, 037503 (2002)
26. G.A. Schuler, R. Vogt, Phys. Lett. B **387**, 181 (1996)
27. R. Gavai et al., Int. J. Mod. Phys. A **10**, 3043 (1995)
28. B.L. Combridge, Nucl. Phys. B **151**, 429 (1979)
29. D.M. Alde et al., Phys. Rev. Lett. **64**, 2479 (1990); D.M. Alde et al., Phys. Rev. Lett. **66**, 133 (1991); D.M. Alde et al., Phys. Rev. Lett. **66**, 2285 (1991)
30. See, e.g., M.J. Leich et al., Nucl. Phys. A **544**, 197c (1992)
31. S.R. Klein, R. Vogt, Phys. Rev. Lett. **91**, 142301 (2003)
32. K.J. Eskola, V.J. Kolhinen, C.A. Salgado, Eur. Phys. J. C **9**, 61 (1999); K.J. Eskola, V.J. Kolhinen, P.V. Ruuskanen, Nucl. Phys. B **535**, 351 (1998)
33. Yu.L. Dokshitzer. Sov. Phys. JETP **46**, 641 (1977); G. Altarelli, G. Parisi, Nucl. Phys. B **126**, 298 (1977); V.N. Gribov, L.N. Lipatov, Sov. J. Nucl. Phys **15**, 438 (1972)
34. R. Vogt, Phys. Rev. C **61**, 035203 (2000)
35. A.L. Ayala, M.B. Gay Ducati, E.M. Levin, Nucl. Phys. B **493**, 305 (1997); Nucl. Phys. B **511**, 355 (1998)
36. I. Balitsky, Nucl. Phys. B **463**, 99 (1996); Y. Kovchegov, Phys. Rev. D **60**, 034008 (2000)
37. A. Ayala, M.B. Gay Ducati, E.M. Levin, Phys. Lett. B **388**, 188 (1996)
38. M.A. Betemps, High density effects in Drell–Yan process at high energies, Master Sciences Dissertation, IF-UFRGS, Porto Alegre (2002) (in portuguese); M.A. Betemps, M.B. Gay Ducati, A.L. Ayala Filho, in Proceedings of VIII International Workshop on Hadrons Physics 2002, p. 319
39. N. Armesto et al., Eur. Phys. J. C **29**, 531 (2003)
40. F. Gelis, J. Jalilian-Marian, Phys. Rev. D **67**, 074019 (2003)
41. M. Glück, E. Reya, A. Vogt, Z. Phys. C **67**, 433 (1995)
42. H. Satz, K. Sridhar, Phys. Rev. D **50**, 3557 (1994)
43. L.F. Mackedanz, J/Ψ suppression in proton–nucleus and nucleus–nucleus processes due to high density effects, Master Sciences Dissertation, IF-UFRGS, Porto Alegre (2003) (in portuguese)
44. B. Anderson et al. [Small x Collaboration], Eur. Phys. J. C **25**, 77 (2002)
45. B. Kopeliovich, A. Tarasov, J. Hüfner, Nucl. Phys. A **696**, 669 (2001)
46. A.K. Chaudhuri, Phys. Rev. Lett. **85**, 232302 (2002)
47. S.J. Brodsky, A.H. Mueller, Phys. Lett. B **206**, 685 (1988)
48. J. Qiu, J.P. Vary, X. Zhang, Nucl. Phys. A **698**, 571 (2002)
49. H. Fujii, Phys. Rev. C **67**, 031901 (2003)
50. R.J. Fries, Phys. Rev. D **68**, 074013 (2003)
51. P. Cortese et al. [NA50 Collaboration], Nucl. Phys. A **715**, 679 (2003)